

ISSN: 2658–5782

Номер 2

2021

МНОГОФАЗНЫЕ СИСТЕМЫ

mfs.uimech.org





A finite volume mesh with periodic boundary conditions for a vortex tube numerical simulation

Mikhaylenko C.I.

Mavlyutov Institute of Mechanisc UFRC RAS, Ufa, Russia

The article describes some aspects of computational modeling of air dynamics in a vortex tube channel. In particular, possible approaches to the numerical study of various geometric parameters are considered, both for the efficiency of temperature stratification and for maximizing or minimizing various parameters of physical diaphragms. An approach to the choice of a method for constructing a finite-volume mesh is presented. It is shown that the best performance can be achieved when using an orthogonalized hexagonal grid with a distribution of finite dimensions close to uniform. The findings are applied in modeling in the OpenFOAM environment for $k - \varepsilon$ and $k - \omega$ turbulence models. It is shown that in the above formulation of the problem, the results obtained demonstrate the general nature of the dependence of the physical parameters on the dimensions of the cold diaphragm. However, a quantitative difference in the results for the $k - \varepsilon$ and $k - \omega$ models should be noted. It requires further research and comparison with experimental data.

Ключевые слова: numerical simulation, finite volume mesh, vortex tube, OpenFOAM

1. Introduction

A vortex tube is a device without moving parts, which divides the gas flow inletting tangentially in the area of one of the tube ends (swirler) into two low pressure swirling flows with temperatures above and below the initial one. Gas under high pressure inlets the vortex tube tangentially through the swirler nozzles, which increases the angular velocity and, therefore, organizes the vortex effect. Then the gas leaves the device through two outlets: a hot diaphragm located along the outer radius at the end farthest from the swirler, and a cold diaphragm forming a nozzle along the channel axis near the swirler. The described design of the vortex tube is called counterflow. Thus, the gas is conventionally divided into two layers. Gas closer to the axis is at a low temperature and exits through the cold diaphragm, while gas at the periphery of the pipe is at a high temperature and exits the device through the hot diaphragm.

The temperature difference caused by the vortex

flow was first discovered by the French engineer Georges J. Ranque in 1931 [1] in the process of improving cyclone pipes for cleaning gases from dust. Later, the German physicist Rudolf Hilsch [2] published research on improving the design of a vortex tube. Subsequently, such vortex tubes were called Rank–Hilsch vortex tubes.

The vortex tube has the following advantages over conventional cooling devices: simplicity of design, no moving parts, operation without electricity and chemicals, small size and light weight, low cost, maintenance-free, instant operation, durability, adjustable temperature [3]. But low thermal efficiency is one of the main limiting factors in the widespread use of vortex tubes. In addition to the indicated disadvantage, it should be noted the increased noise level and the issue of the availability of compressed gas, which can also limit the application. Therefore, when compactness, reliability and lower cost of equipment are the main factors, and high operating efficiency is less important, the vortex tube becomes a good device for heating or cooling gas, purifying and dehydrating gas, separating gas mixtures, applying

DNA, liquefying natural gas and for other purposes [4–6].

Due to the simplicity of the device and its reliability, vortex tubes are widely used in many industries. Vortex tubes are used as refrigeration units in the food industry, for drying and separating gas in the oil industry, for monitoring the environment in the study of underwater environments [7], for heating and cooling chemicals [8], etc.

The main physical mechanism of the processes that determine gas cooling in a vortex tube has not yet been fully studied. There is continue investigations of the emerging effect and attempts to explain this phenomenon. So, in works [9, 10] reviews of existing models of vortex tubes and their designs are given. The existing theories are described and new approaches to explaining the Rank–Hilsch effect are presented.

It is also necessary to highlight a large number of experimental studies in the area of the design and dimensions of the vortex tube. The work [11] presents the results of a study of the efficiency of cooling a vortex tube taking into account the number of nozzle holes. The authors of the article [12] propose a more detailed consideration of the geometric parameters of the pipe, such as pipe length, diameter and internal taper angle, as well as their influence on the efficiency of the pipe. Thus, there are experimental studies suggesting characteristic pipe parameters and feed gas properties.

This work describes the development of a finite-volume mesh focused on doing massive computational experiments to study the dynamics of gas in the channel of a vortex tube. Possible limitations imposed by spatial decomposition in parallel calculations using MPI technology are taken into account. Several ways to prepare a mesh for calculations in the OpenFOAM software are described below. In this case, the experience [13–15] obtained earlier is used. Also, when developing the mesh, the features of the possible influence of the boundary conditions on the results obtained are taken into account [16].

2. The mathematical model

2.1. The common hydrodynamics model

The hydrodynamics processes into a vortex tube channel can be described by the standard system of continuous media equations contents of the continuity equation, the equation of impulses, the energy conservation equation and closure the system by an equation of state.

- The continuity equation

$$\frac{\partial \rho}{\partial t} + \frac{\partial \rho u_i}{\partial x_i} = 0.$$

- The equation of impulses (Navier–Stokes equation)

$$\frac{\partial \rho u_j}{\partial t} + \frac{\partial \rho u_j u_i}{\partial x_i} = -\frac{\partial p}{\partial x_j} + \frac{\partial \tau_{ji}}{\partial x_i}.$$

- The energy conservation equation

$$\frac{\partial \rho E}{\partial t} + \frac{\partial \rho u_i E}{\partial x_i} = -\frac{\partial p u_i}{\partial x_i} + \frac{\partial \tau_{ji} u_i}{\partial x_j}.$$

- The equation of state of an ideal gas

$$e = \frac{p}{(\gamma - 1)\rho}.$$

The following notation is here: ρ is the gas density; u_i are the velocity vectors components; p is the pressure; E is the specific total energy of gas; γ is the adiabatic exponent; e is the specific internal energy linked with the specific total energy by equation

$$E = e + \frac{\sum_i u_i^2}{2};$$

τ_{ji} is the viscous stress tensor calculated as

$$\tau_{ji} = \mu \left[\left(\frac{\partial u_j}{\partial x_i} + \frac{\partial u_i}{\partial x_j} \right) - \frac{2}{3} \delta_{ij} \frac{\partial u_k}{\partial x_k} \right],$$

μ is the dynamic viscosity and δ_{ij} is the Kronecker symbol.

When using the turbulence model, μ is calculated as $\mu = \mu_0 + \nu_t \rho$, where μ_0 is the dynamic viscosity of gas and ν_t is a kinematic eddy viscosity calculated by any turbulence model.

2.2. The $k - \omega$ turbulence model

The turbulence model $k - \omega$ is considered one of the best for the case when there is a solid wall in the computational domain. The vortex tube corresponds to this case. The model is described by the turbulence energy equation and the specific dissipation rate equation.

- The turbulence energy equation

$$\begin{aligned} \frac{\partial k}{\partial t} + \frac{\partial u_i k}{\partial x_i} &= \\ &= \tau_{ji} \frac{\partial u_j}{\partial x_i} - \beta^* \omega k + \frac{\partial}{\partial x_i} \left[(\nu + \sigma^* \nu_t) \frac{\partial k}{\partial x_i} \right]. \end{aligned}$$

- The specific dissipation rate equation

$$\begin{aligned} \frac{\partial \omega}{\partial t} + \frac{\partial u_i \omega}{\partial x_i} &= \\ &= \frac{\alpha \omega}{k} \tau_{ji} \frac{\partial u_j}{\partial x_i} - \beta^* \omega^2 + \frac{\partial}{\partial x_i} \left[(\nu + \sigma \nu_t) \frac{\partial \omega}{\partial x_i} \right]. \end{aligned}$$

Here k is the turbulence energy; ω is the specific dissipation rate; ν is the kinematic viscosity of gas; ν_t is the kinematic eddy viscosity calculated as

$$\nu_t = \frac{k}{\omega};$$

and closure coefficients are empirical values

$$\alpha = \frac{13}{25}, \quad \beta = \frac{9}{125}, \quad \beta^* = \frac{9}{100}, \quad \sigma = \sigma^* = \frac{1}{2}.$$

2.3. The $k - \varepsilon$ turbulence model

The $k - \varepsilon$ turbulence model is known as more simple in its numerical realization. The model equations are the turbulence energy equation and the turbulence dissipation rate equation.

- The turbulence energy equation

$$\begin{aligned} \frac{\partial k}{\partial t} + \frac{\partial u_i k}{\partial x_i} &= \\ &= \frac{\partial}{\partial x_i} \left[\left(\nu + \frac{\nu_t}{\sigma_k} \right) \frac{\partial k}{\partial x_i} \right] - \frac{2}{3} k \frac{\partial u_i}{\partial x_i} - \rho \varepsilon. \end{aligned}$$

- The turbulence dissipation rate equation

$$\begin{aligned} \frac{\partial \varepsilon}{\partial t} + \frac{\partial u_i \varepsilon}{\partial x_i} &= \\ &= \frac{\partial}{\partial x_i} \left[\left(\nu + \frac{\nu_t}{\sigma_\varepsilon} \right) \frac{\partial \varepsilon}{\partial x_i} \right] - \frac{2}{3} C_1 \varepsilon \frac{\partial u_i}{\partial x_i} - C_2 \frac{\varepsilon^2}{k}. \end{aligned}$$

Here k is the turbulence energy; ε is the turbulence dissipation rate; ν is the kinematic viscosity of gas; ν_t is the kinematic eddy viscosity calculated as

$$\nu_t = C_\mu \frac{k^2}{\varepsilon};$$

and the model empirical closure coefficients are values

$$C_1 = 1.44, \quad C_2 = 1.92, \quad \sigma_k = 1, \quad \sigma_\varepsilon = 1.3.$$

2.4. The initial and boundary conditions

A counter flow vortex tube is considered in the work is a cylindrical device which has four tangentially placed inlet channels and two outlet diaphragms. The main channel length of a simulated tube is 120 mm and the diameter equal to 16 mm. The diameter of the cold diaphragm changes from wthe size equal to 5 mm to 11 mm. The hot diaphragm placed near external wall of cylinder is circular and its wide equal to 0.5 mm. The outlets of the computational domain are located at the ends of the cylinder, which has the diameter equal to diameter of main cylinder, and places at a certain distance from the outlet diaphragms.

The initial conditions is close to normal ones. The velocity of gas equal to zero, the temperature equal to

293 K, the pressure equal to atmospheric (100 kPa) and the density equal to air density for ordinal conditions.

Inlet parameters are constant pressure equal to 600 kPa (6 atm) and constant temperature (293 K). An inlet velocity is determined by the pressure gradient.

Outlet parameters are the normal pressure (100 kPa), and flow boundary conditions for a velocity and a temperature.

The boundary conditions for the physical parameters on the wall are determined by the turbulence model. Where are set the slip boundary condition for the $k - \varepsilon$ turbulence model case and the no-slip ones for the $k - \omega$ model. The boundary conditions for turbulence parameters on the wall describes by corresponding wall functions.

3. A mesh construction

A vortex tube is a complex geometrical area, since in addition to the main cylindrical channel, there are also swirler inlets, outlet diaphragms and boundaries with outlet conditions, placed with the necessary requirements. The simplest option for meshing for complex areas is automatic generation. OpenFOAM allows to use the unstructured mesh automatically generated in the Salome software. The second option is to generate a pseudo-structured orthogonalized mesh using the SnappyHexMesh utility included in the OpenFOAM software.

3.1. Automatically generated meshes

Previously the author investigated the possibility of using an automatically generated unstructured mesh with finite octahedral volumes [14]. Fig. 1 shows an example of such a mesh created with Salome. It should be noted that despite the uniformity of such a mesh on the surface, as shown in Fig. 1 (a) and (c), the mesh does not have sufficient uniformity inside, as can be clearly seen in Fig. 1 (b). Such a structure of a finite-volume mesh leads to a slight increase in the computational error.

The most significant disadvantages of such a finite-volume mesh are as follows. With the number of nodal points comparable to that of a hexagonal mesh, the number of faces between neighbour finite volumes for an unstructured mesh increases significantly. Since the finite volume method calculates the flow of physical values through each face, the simulation time increases significantly. The next important disadvantage is the non-orthogonal of the unstructured mesh, which in the general case also leads to an increase in the simulation time and, in addition, to an increase in the error. The last significant disadvantage is the fact that the unstructuredness of the mesh complicates the spatial decomposition procedure, which increases the

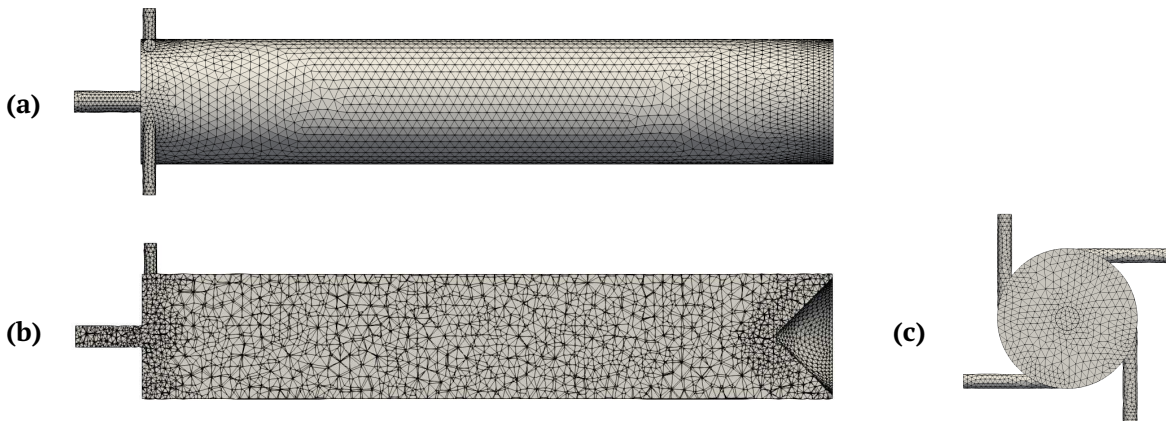


Figure 1. The mesh generated by Salome: general view along the tube (a); cross-section of the mesh (b); view from the side of the cold diaphragm (c)

simulation time on the computational cluster.

Thus, the relative ease of constructing an unstructured mesh is largely lost by its general disadvantages.

The issue of automatic mesh generation with a small number of finite volumes using OpenFOAM [15] was also considered earlier. The SnappyHexMesh utility is intended for this goal. The mesh is created using 3D reference geometry described in STL format. The utility allows to get a partially structured orthogonalized and mostly hexagonal mesh.

The main disadvantage of this method of generating a mesh is that if the number of nodal points is limited, the resulting mesh is highly homogeneous with artifacts and concentrations.

Fig. 2 shows an example of a mesh generated by

the SnappyHexMesh utility. It should be noted that the number of node points on this mesh is comparable to the number of nodes on the unstructured mesh shown in Fig. 1. The figure shows that such a mesh is fairly uniform on the surface and in depth. However, in the near-wall areas and in the places of surface bends, a considerable concentration of the nodal points is observed, which is clearly visible in Fig. 2 (b) and (c).

It should be noted that in the case presented in Fig. 2, the computational process is completely impossible, since to supply stability, it is necessary to set the time step much less than any reasonable value.

It is possible to achieve computational stability on such a finite-volume mesh if we make it more uniform, but this significantly increases the number of nodal

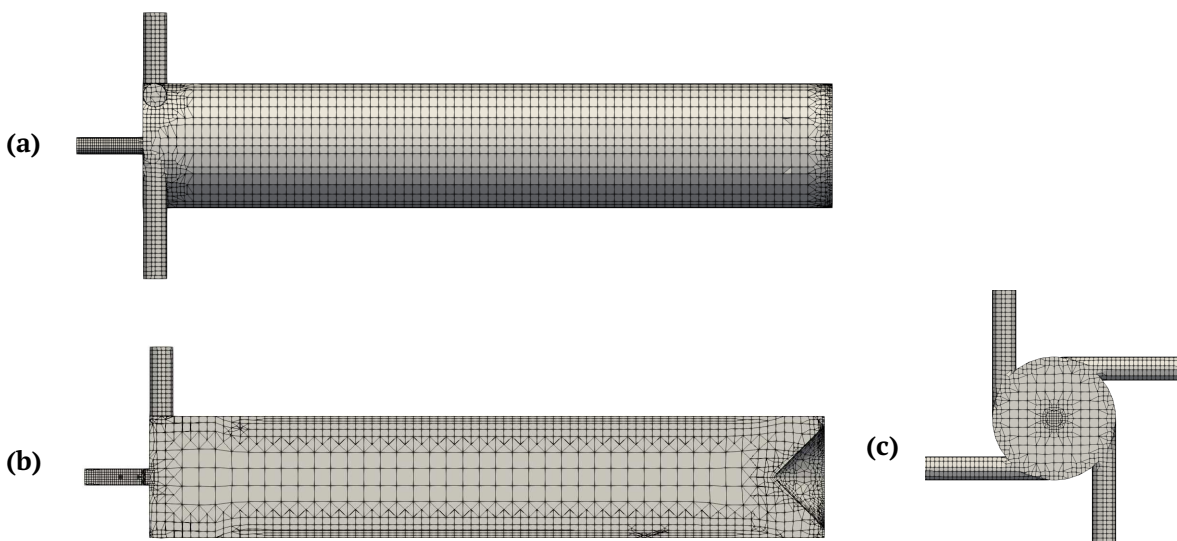


Figure 2. The mesh generated by SnappyHexMesh utility: general view along the tube (a); cross-section of the mesh (b); view from the side of the cold diaphragm (c)

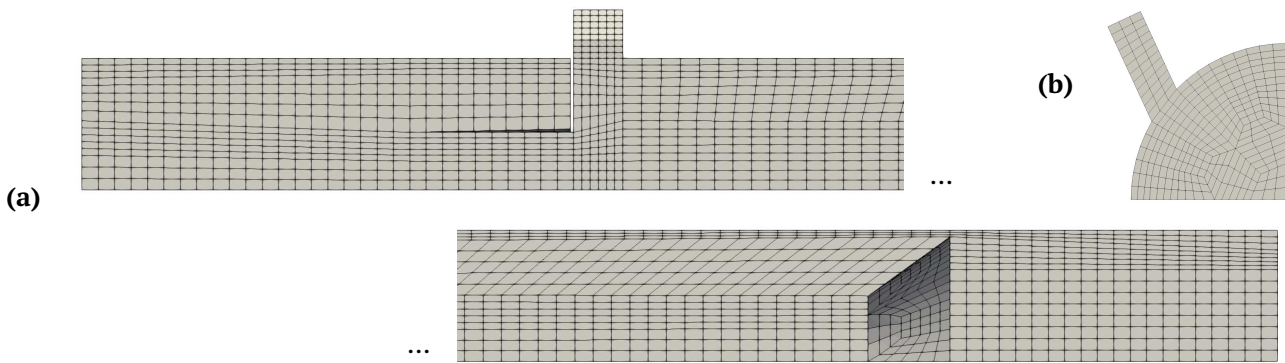


Figure 3. The manually made mesh for using with $k - \epsilon$ turbulence model: the cold diaphragm and the hot diaphragm areas (a) and view from the side of the cold diaphragm (b)

points, which ultimately dramatically increases the simulation time.

3.2. Manually created meshes

We can try to avoid the problems described in the previous section by building a finite-volume mesh using the blockMesh utility included in the OpenFOAM software. The utility uses a formal description to divide the computational domain into a set of non-intersecting blocks (boxes) but contacting with their faces, each of which will contain its own orthogonal hexagonal grid of finite volumes. The specified description is written in a special dictionary file blockMeshDict. The dictionary contains the coordinates of the points that will be the corner points of the hexagonal blocks; descriptions of possible curves between two points, if this edge is not a straight line. The dictionary also contains definitions of blocks and the way they will be split into finite volumes. In addition, surfaces are selected in the dictionary, on which boundary conditions will be set.

The computational domain describing the vortex tube channel is very difficult for manual development

of a uniform hexagonal finite-volume mesh. The complexity is determined by several factors. First, one can distinguish at least three nested cylindrical regions oriented along the channel. The mesh for the inner cylinder is easily obtained using the five-area method. However, for the outer cylinder, some action must be taken to maintain the relative uniformity of the mesh. For this it is necessary to introduce additional blocks, as can be seen in Fig. 3 (b) and 4 (b). Then it is necessary to describe the hot diaphragm (third cylinder), which has a very small thickness and, in addition, a cone-shaped plug is located at this end of the vortex tube.

The above problems can be partially solved. The result shown in Fig. 3 shows a finite volume mesh designed for the computational domain with the constraints described above. This mesh is intended for calculations using the $k - \epsilon$ turbulence model. In the case of using the $k - \epsilon$ model, on the wall it is possible to set the condition of no-slip and not select the near-wall layer, as can be seen in the figure.

The main significant difference in the use of a computational mesh constructed in this way from

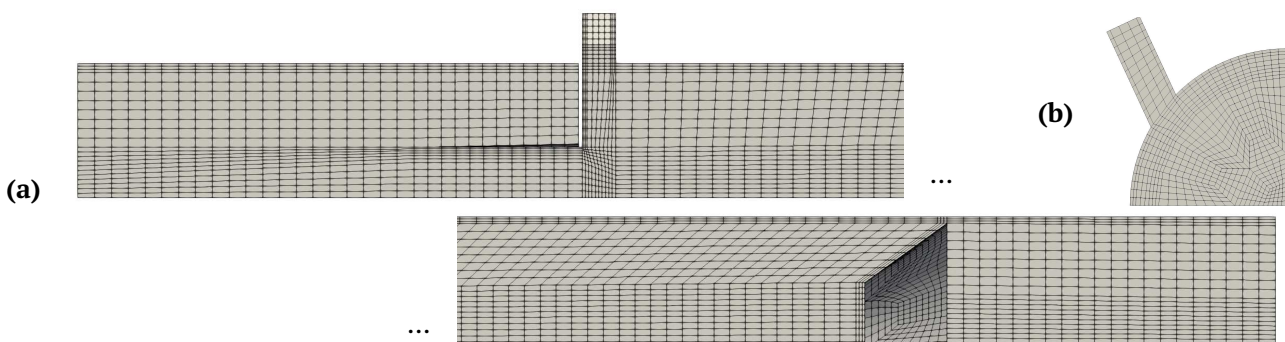


Figure 4. The manually made mesh for using with $k - \omega$ turbulence model: the cold diaphragm and the hot diaphragm areas (a) and view from the side of the cold diaphragm (b)

an unstructured mesh is significantly less simulation time. In addition, a difference in the level of computational error is assumed, but this issue has not been checked for the case of modeling a vortex tube using these meshes.

When constructing a mesh for modeling using a $k - \omega$ turbulence model, an additional requirement arises to select several layers of finite volumes of the near-wall region. It should be noted that the method of constructing the computational mesh, which was used for calculations with the $k - \varepsilon$ turbulence model, is fully applicable for this case as well. The definition of boxes in the blockMeshDict dictionary allows to set the non-uniformity of the finite-volume mesh, which makes it possible to select the near-wall layer. In Fig. 4 shows a mesh created with such modifications. It is worth noting that such a mesh contains almost twice as many finite volumes as compared to the mesh shown in Fig. 3.

4. Some results

Finite-volume meshes described in section 3.2. have proven themselves well in calculations using the sonicFoam solver from the OpenFOAM software [18–20]. These meshes are now actively used in massive computational experiments.

Fig. 5 shows the dependence of the time-average temperature at the outlet of the cold diaphragm nozzle on the diameter of the cold diaphragm. Below are the results obtained by the time of this writing on the study of the dependence of various physical parameters on the diameter of the cold diaphragm. When simulating the vortex tube has the following main dimensions: channel diameter $D = 16$ mm; channel length $L = 120$ mm; cold nozzle length $l = 20$ mm; the

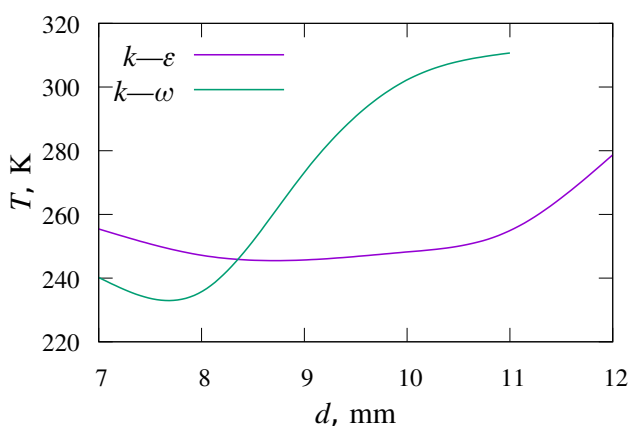


Figure 5. Dependence of the time-average temperature at the outlet of the nozzle of the cold diaphragm on the diameter of the cold diaphragm

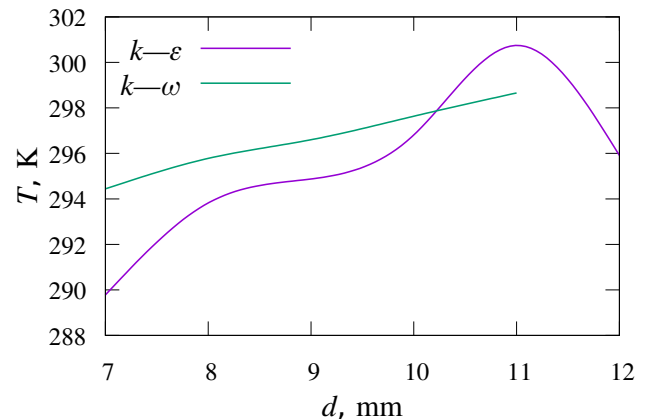


Figure 6. Dependence of the time-average temperature at the outlet of the hot diaphragm on the diameter of the cold diaphragm

diameter of the cold diaphragm varied from $d = 7$ mm to $d = 12$ mm. Data are given for calculations using $k - \varepsilon$ and $k - \omega$ turbulence models. In the figure, you can see that for both options, the allocation of a certain conditionally optimal diameter is characteristic, at which the temperature of the outgoing air is minimal. However, the specified minimum is reached at different values of the diameter and has different values of temperature.

It follows from the literature that for these geometrical parameters, the values obtained in the $k - \omega$ turbulence model are closer to the experimental data [21], but this statement requires additional verification in the case under consideration.

In Fig. 6 shows the dependence of the average temperature on the hot diaphragm on the diameter of the cold diaphragm. These plots show a fairly similar relationship for both turbulence models. However, in the future, it is necessary to expand the range of variation of the cold diaphragm diameter in order to explain the maximum observed when using the $k - \varepsilon$ turbulence model.

5. Conclusion

Thus, it is shown that the construction of a computational mesh using the blockMesh utility allows to create a better mesh due to human participation. Despite the fact that in some parts of the computational domain such a mesh deviates slightly from the real geometry of the vortex tube, as it happened for the swirlers in Fig. 3 and 4, this has no noticeable effect on the result.

A particularly important property of the mesh created by the blockMesh utility is the ability to extensively control the size of individual finite volumes, their placement, uniformity and condensation.

It should also be noted that the language for describing the dictionary `blockMeshDict` allows to widely enter and use variables, as well as use arithmetic expressions in the C language. To calculate these expressions, the C compiler is called. Thanks to this possibility, the creation and modification of the computational mesh can be largely automated. This fact makes it easier to carry out massive computational experiments.

Thus, the `blockMesh` utility can be recognized as one of the most convenient and accurate tools for creating a finite-volume mesh for modeling a vortex tube in the OpenFOAM software.

References

- [1] Ranque G.J. Experiments on expansion a vortex with Simultaneous Exhaust of hot air and cold air // *J. Phys. Radium*. 1994. V. 4. Pp. 112S–114S. (in French)
- [2] Hilsch R. The Use of the Expansion of Gases in a Centrifugal Field as Cooling Process // *Review of Scientific Instruments*. 1947. V. 18. Pp. 108–113.
DOI: [10.1063/1.1740893](https://doi.org/10.1063/1.1740893)
- [3] Khodorkov L., Poshernev N.V., Zhidkov M.A. The vortex tube: a universal device for heating, cooling, cleaning, and drying gases and separating gas mixtures // *Chemical and Petroleum Engineering*. 2003. V. 39. Pp. 409–415.
DOI: [10.1023/A:1026336813155](https://doi.org/10.1023/A:1026336813155)
- [4] Ebmeier R., Whitney S., Alugupally S., Nelson M., Padhye N., Gogos G., Viljoen H.J. Ranque–Hilsch Vortex Tube Thermocycler for DNA Amplification // *Instrumentation Science & Technology*. 2004. V. 32. Pp. 567–570.
DOI: [10.1081/CI-200029810](https://doi.org/10.1081/CI-200029810)
- [5] Boucher R.F., Tippetts J.R. Vortex-tube-driven thermo-electricity // In *Sixth triennial international symposium on Fluid Control, Measurement and Visualization*, 6th, Sherbrooke, Canada. 2000. Paper 50.
- [6] Westley R. A Bibliography and Survey of The Vortex Tube // *The College of Aeronautics*. 1957.
- [7] Baz A., Gilheany J., Kalvitas A. Feasibility of vortex tube assisted environmental control of an underwater research habitat // *Ocean Eng.* 1987. V. 15. Pp. 34–54.
DOI: [10.1016/0029-8018\(88\)90018-2](https://doi.org/10.1016/0029-8018(88)90018-2)
- [8] Bruno T.J. Laboratory applications of the vortex tube // *Journal of Chemical Education*. 1987. V. 64. Pp. 987–988.
DOI: [10.1021/ed064p987](https://doi.org/10.1021/ed064p987)
- [9] Gutsol A.F. The Ranque effect // *Physics-Uspexhi*. 1997. V. 40. Pp. 639–658.
DOI: [10.1070/PU1997v040n06ABEH000248](https://doi.org/10.1070/PU1997v040n06ABEH000248)
- [10] Eiamsa-Ard S., Promvong P. Review of Ranque–Hilsch effects on vortex tubes // *Renewable and Sustainable Energy Reviews*. 2008. V. 1. Pp. 1822–1842.
DOI: [10.1016/j.rser.2007.03.006](https://doi.org/10.1016/j.rser.2007.03.006)
- [11] Attalla M., Ahmed H., Ahmed M.S., El-Wafa A.A. An experimental study of nozzle number on Ranque–Hilsch counter-flow vortex tube // *Experimental Thermal and Fluid Science*. 2017. V. 82. Pp. 381–389.
DOI: [10.1016/j.expthermflusci.2016.11.034](https://doi.org/10.1016/j.expthermflusci.2016.11.034)
- [12] Hamdan M.O., Al-Omari S.-A., Oweimer A.S. Experimental study of vortex tube energy separation under different tube design // *Experimental Thermal and Fluid Science*. 2018. V. 91. Pp. 306–311.
DOI: [10.1016/j.expthermflusci.2017.10.034](https://doi.org/10.1016/j.expthermflusci.2017.10.034)
- [13] Mikhaylenko C.I. Simulation of the vortex tube: design of a hexagonal mesh for computational experiments in OpenFOAM // *Proceedings of the Mavlyutov Institute of Mechanics*. 2016. V. 11. Pp. 112–118. (in Russian)
DOI: [10.21662/uim2016.1.017](https://doi.org/10.21662/uim2016.1.017)
- [14] Minishev Sh.R., Mikhailenko C.I. Formation of an unstructured mesh for a vortex tube model in OpenFOAM with Salome // In the book: *Physicochemical hydrodynamics: models and applications. Abstracts of the Second All-Russian Summer School-Conference*. 2018. (in russian)
- [15] Koroleva E.N., Mikhailenko C.I. Constructing the geometry of the calculation domain for the vortex tube model by SnappyHxMesh utility of the OpenFOAM software // In the book: *Physicochemical hydrodynamics: models and applications. Abstracts of the Second All-Russian Summer School-Conference*. 2018. (in russian).
- [16] Minibaev M.R., Mikhaylenko C.I. Investigation of the influence of boundary conditions in the numerical solution of a vortex tube model // *Multiphase Systems*. 2019. V. 14. Pp. 89–100. (in Russian)
DOI: [10.21662/mfs2019.2.013](https://doi.org/10.21662/mfs2019.2.013)
- [17] Mikhaylenko C.I. Making of a finite-difference mesh and a turbulence model selection for a numerical simulations of a vortex tube in OpenFOAM software // *Journal of Physics: Conference Series*. 2020. V. 1677. 012021.
DOI: [10.1088/1742-6596/1677/1/012021](https://doi.org/10.1088/1742-6596/1677/1/012021)
- [18] Mikhaylenko C.I. Vortex tube modelling: outlet parameter dependencies of cold air production // *Journal of Physics: Conf. Series*. 2019. V. 1158. 032032.
DOI: [10.1088/1742-6596/1158/3/032032](https://doi.org/10.1088/1742-6596/1158/3/032032)
- [19] Adullin B.R., Mikhaylenko C.I. Influence of the channel length of a vortex tube on the air temperature separation // *Journal of Physics: Conf. Series*. 2019. V. 1268. 012001.
DOI: [10.1088/1742-6596/1268/1/012001](https://doi.org/10.1088/1742-6596/1268/1/012001)
- [20] Privalov L.Y., Mikhaylenko C.I. The effect of an additional air inlet in the hot outlet area on the overall effectiveness of a vortex tube // *Journal of Physics: Conference Series*. 2019. V. 1392. 012019.
DOI: [10.1088/1742-6596/1392/1/012019](https://doi.org/10.1088/1742-6596/1392/1/012019)
- [21] Burazer J.M.; Čočić A.S., Lečić M.R. Numerical research of the compressible flow in a vortex tube using OpenFOAM software // *Thermal Science*. 2017. V. 21. Pp. S745–S758.
DOI: [10.2298/TSC1160223195B](https://doi.org/10.2298/TSC1160223195B)